Received: 20 March 2024 | Accepted: 22 April 2024

DOI: 10.1111/age.13441

RESEARCH ARTICLE

ANIMAL GENETICS WILEY

# Intragenic *MFSD8* duplication and histopathological findings in a rabbit with neuronal ceroid lipofuscinosis

**Matthias Christen**[1] | **Katharina M. Gregor**[2] | **Ariane Böttcher-Künneke**[3] | **Mara S. Lombardo**[2] | **Wolfgang Baumgärtner**[2] | **Vidhya Jagannathan**[1] | **Christina Puff**[2] | **Tosso Leeb**[1]

[1]Institute of Genetics, Vetsuisse Faculty, University of Bern, Bern, Switzerland

[2]Department of Pathology, University of Veterinary Medicine Hannover, Hannover, Germany

[3]Animal Clinic Brunautal GbR, Bispingen, Germany

**Correspondence**
Tosso Leeb, Institute of Genetics, Vetsuisse Faculty, University of Bern, 3001 Bern, Switzerland.
Email: tosso.leeb@unibe.ch

**Abstract**

Neuronal ceroid lipofuscinoses (NCL) are among the most prevalent neurodegenerative disorders of early life in humans. Disease-causing variants have been described for 13 different NCL genes. In this study, a refined pathological characterization of a female rabbit with progressive neurological signs reminiscent of NCL was performed. Cytoplasmic pigment present in neurons was weakly positive with Sudan black B and autofluorescent. Immunohistology revealed astrogliosis, microgliosis and axonal degeneration. During the subsequent genetic investigation, the genome of the affected rabbit was sequenced and examined for private variants in NCL candidate genes. The analysis revealed a homozygous ~10.7 kb genomic duplication on chromosome 15 comprising parts of the *MFSD8* gene, NC_013683.1:g.103,727,963_103,738,667dup. The duplication harbors two internal protein coding exons and is predicted to introduce a premature stop codon into the transcript, truncating ~50% of the wild-type *MFSD8* open reading frame encoding the major facilitator superfamily domain containing protein 8, XP_002717309.2:p.(Glu235Leufs*23). Biallelic loss-of-function variants in *MFSD8* have been described to cause NCL7 in human patients, dogs and a single cat. The available clinical and pathological data, together with current knowledge about *MFSD8* variants and their functional impact in other species, point to the *MFSD8* duplication as a likely causative defect for the observed phenotype in the affected rabbit.

**KEYWORDS**

animal model, Batten disease, hereditary disease, neurology, *Oryctolagus cuniculus*, precision medicine

## INTRODUCTION

Lysosomal storage diseases (LSD) are a large and heterogeneous group of inherited metabolic disorders. Defects that impair proper lysosomal function or transport of molecules from and to the lysosome typically lead to accumulation of incompletely degraded substrates, which is the hallmark of LSD (Parenti et al., 2015). Currently, more than 70 LSD with known genetic cause have been documented, mostly with a monogenic autosomal recessive mode of inheritance (Platt et al., 2018). Neuronal ceroid

Matthias Christen and Katharina M. Gregor are co-first authors to this work.

Christina Puff and Tosso Leeb are co-senior authors to this work.

lipofuscinoses (NCL) are a subgroup of LSD with currently 14 known entities in humans. Disease-causing variants have been described in 13 different genes (Nita et al., 2016). Neuronal ceroid lipofuscinoses are among the most prevalent neurodegenerative disorders of early life (Qureshi et al., 2020). They are morphologically characterized by cellular inclusions of ceroid lipopigments, neuronal loss and progressive neurodegeneration. The age of onset and clinical phenotype of NCL may be variable and depends on the specific gene and the specific pathogenic variant(s) involved. Shared clinical features of NCL consist of progressive loss of motor function and mental capabilities. Many NCL additionally involve a progressive loss of vision (Schulz et al., 2013).

During the last two decades, veterinary medicine has made great progress concerning the description and genetic characterization of NCL. Different forms of NCL have been described in many domestic and wild animal species (Barker et al., 2023; Bond et al., 2013; Chalkley et al., 2014; Guo et al., 2019; Huber et al., 2020; Katz et al., 2020; Nicholas et al., 1995; Nittari et al., 2023; Nolte et al., 2016; Swier et al., 2022; Villani et al., 2019). Furthermore, disease-causing genetic variants were discovered or experimentally induced in domestic animals for nine of the 14 different human NCL types (Table 1) (Huber et al., 2020).

This study was initiated following the report of a female rabbit aged 3 years and 11 months with progressive neurological signs reminiscent of NCL. After an initial clinical case description (Böttcher-Künneke et al., 2020), the goal of this study was to further characterize the phenotype of the rabbit by means of histochemistry and immunohistochemistry, as well as to identify a possible underlying genetic defect.

## MATERIALS AND METHODS

### Animal selection

The described analyses and experiments were performed on samples derived from a female lionhead dwarf rabbit that has been described previously in a preliminary case report (Böttcher-Künneke et al., 2020). The rabbit showed various neurological signs and behavioral changes including progressive anxiety at noises, light stimuli or touch with consecutive self-traumatization through uncontrolled movement, hyperesthesia, disorientation, ataxia, stereotypical head movements, phantom scratching, compulsive wandering, epileptic seizures, progressive loss of vision to blindness, temporary dyspnea and intermittent cessation of food and water intake.

The sire of the affected rabbit did not show comparable neurological disease signs. The sire was euthanized at ≥6 years of age in the course of an unrelated disease and subsequently examined pathomorphologically. Skin, lung, liver, spleen and kidney samples of the sire were available for genotyping of the identified candidate variant. Unaltered tissue from the central nervous system from a young adult male chinchilla bastard rabbit of approximately 6 months of age, which was part of an unrelated study, served as a representative positive control for immunohistology.

### Histochemistry and immunohistology

Tissue samples were fixed in 10% neutral buffered formalin for 24 h and embedded in paraffin wax. Tissue sections of 2–4 μm thickness were stained with hematoxylin–eosin and examined using light microscopy. In addition, sections of central nervous system (CNS) were subjected to Sudan black B (Robles, 1978) and Ziehl Neelsen (Ziehl, 1882) staining. In the case of the female affected rabbit, unstained sections of CNS, including cerebral cortex, hippocampus, diencephalon, cerebellum, brainstem, cervical, thoracic and lumbar spinal cord, were further examined by fluorescence microscopy to identify lipofuscin pigments.

Immunohistology was performed on 2–4 μm thick tissue sections of the CNS using the avidin-biotin-peroxidase complex (#PK 6100, Vectastain elite ABC kit; Vector Laboratories, Burlingame, CA, USA) and 3,3′-diaminobenzidine tetrahydrochloride (0.05%; Sigma-Aldrich Chemie GmbH) as previously published (Huang et al., 2021). The pretreatments and dilutions of the antibodies used are listed in Table 2. Unaltered CNS tissue from a chinchilla bastard rabbit served as representative positive control.

Tissue sections were examined by two or three pathologists using a light microscope (Olympus BX53; Olympus Europa SE & Co. KG, Hamburg, Germany). Autofluorescence was tested with a BZ-9000E microscope (Keyence Deutschland GmbH, Neu-Isenburg, Germany) using blue (DAPI filter, excitation 377 ± 50 nm, emission 477 ± 60 nm) and green filters (GFP filter, excitation 472.5 ± 30 nm, emission 520 ± 35 nm).

### Whole-genome sequencing

Genomic DNA was isolated from a tissue sample of the affected female rabbit with the Maxwell RSC Tissue Kit using a Maxwell RSC instrument (Promega, Dübendorf, Switzerland). An Illumina TruSeq PCR-free DNA library with ~420 bp insert size was prepared. A total of 235 million 2 × 150 bp paired-end reads on a NovaSeq 6000 instrument were obtained (22.4× coverage). Mapping to the OryCun2.0 reference genome assembly was performed as described (Jagannathan et al., 2019). The sequence data were deposited under the study accession PRJEB28783 and the sample accession SAMEA6488642 at the European Nucleotide Archive.

**TABLE 1** Overview of Neuronal ceroid lipofuscinose (NCL) types and known genetic causes in humans and domestic animals. OMIM (Amberger et al., 2015) and OMIA (Nicholas et al., 1995) identifiers are given.

| Human disease designation | Gene | Protein | Species | OMIM/OMIA |
|---|---|---|---|---|
| CLN1 | *PPT1* | Palmitoyl protein thioesterase 1 | Human | 256730 |
| | | | Dog | 001504-9615 |
| | | | Sheep | 001504-9940 |
| CLN2 | *TPP1* | Tripeptidyl peptidase 1 | Human | 204500 |
| | | | Dog | 001472-9615 |
| | | | Pig | 001472-9823 |
| CLN3 | *CLN3* | CLN3 lysosomal/endosomal transmembrane protein, battenin | Human | 204200 |
| | | | Pig | 002432-9823 |
| CLN4A | *CLN6* | CLN6 transmembrane ER protein | Human | 204300 |
| CLN4B | *DNAJC5* | DnaJ heat shock protein family (Hsp40) member C5 | Human | 162350 |
| CLN5 | *CLN5* | CLN5 intracellular trafficking protein | Human | 256731 |
| | | | Dog | 001482-9615 |
| | | | Cattle | 001482-9913 |
| | | | Sheep | 001482-9940 |
| CLN6 | *CLN6* | CLN6 transmembrane ER protein | Human | 601780 |
| | | | Dog | 001443-9615 |
| | | | Cat | 001443-9685 |
| | | | Sheep | 001443-9940 |
| CLN7 | *MFSD8* | Major facilitator superfamily domain containing 8 | Human | 610951 |
| | | | Dog | 001962-9615 |
| | | | Cat | 001962-9685 |
| CLN8 | *CLN8* | CLN8 transmembrane ER and ERGIC protein | Human | 600143 |
| | | | Dog | 001506-9615 |
| CLN9 | — | Unknown | Human | 609055 |
| CLN10 | *CTSD* | Cathepsin D | Human | 610127 |
| | | | Dog | 001505-9615 |
| | | | Sheep | 001505-9940 |
| CLN11 | *GRN* | Granulin precursor | Human | 614706 |
| 'CLN12', Kufor-Rakeb syndrome | *ATP13A2* | ATPase cation transporting 13A2 | Human | 606693 |
| | | | Dog | 001552-9615 |
| CLN13 | *CTSF* | Cathepsin F | Human | 615362 |
| 'CLN14', epilepsy, progressive myoclonic 3, with or without intracellular inclusions | *KCTD7* | Potassium channel tetramerization domain containing 7 | Human | 611726 |

The genome sequence data of 12 control rabbits were also included in the analysis (Table S1).

## Variant calling and filtering

Variant calling was performed using GATK HaplotypeCaller (McKenna et al., 2010) in gVCF mode as described previously (Jagannathan et al., 2019). To predict the functional effects of the called variants, SNPEFF (Cingolani et al., 2012) software, together with the OryCun2.0 reference genome assembly and NCBI annotation release 102, was used. Numbering within the rabbit *MFSD8* gene corresponds to the NCBI RefSeq accession numbers XM_002717263.3 (mRNA) and XP_002717309.2 (protein).

## PCR and Sanger sequencing

Primers F2_DupF and R1_DupR were used for the generation of an amplicon containing the junction of the duplication at NC_013683.1:g.103,727,963_103,738,667dup (Table S2). PCR was performed for 30 cycles using the Qiagen Multiplex PCR kit (Qiagen, Hilden, Germany). Product sizes were analyzed on a

**TABLE 2** Antibodies used for immunohistochemistry.

| First antibody | Epitope | Species, clonality | Dilution | Pretreatment | Source | Second antibody |
|---|---|---|---|---|---|---|
| $\beta$-APP | Axonal damage | Mouse, mc | 1:1000 | 20 min microwave, citrate buffer (pH 6.0) | #MAB348, Millipore, Burlington, USA | Goat anti-mouse, 1:200, #BA-9200, Biozol |
| GFAP | Astrocytes | Mouse, mc | 1:800 | None | #G3893, Sigma-Aldrich, Merck, KGaA, Darmstadt, Germany | Goat anti-mouse, 1:200, #BA-9200, Biozol |
| nNF | Neurons, axonal damage | Mouse, mc | 1:1000 | 20 min microwave, citrate buffer (pH 6.0) | #SMI-311, Sternberger Monoclonals Incorporated, MD, USA | Goat anti-mouse, 1:200, #BA-9200, Biozol |
| pNF | Physiological axon structures | Mouse, mc | 1:4000 | none | #SMI-312, Sternberger Monoclonals Incorporated, MD, USA | Goat anti-mouse, 1:200, #BA-9200, Biozol |
| Iba1 | Macrophages, microglia | Goat, pc | 1:400 | 20 min microwave, citrate buffer (pH 6.0) | #011-27991, Fujifilm Wako Pure Chemical Corporation, Osaka, Japan | Horse anti-goat, 1:200, #PI-9500, Vector Laboratories Inc. |

Abbreviations: GFAP, glial fibrillary acidic protein; Iba1, ionized calcium binding adapter molecule 1; mc, monoclonal; nNF, non-phosphorylated neurofilament; pc, polyclonal; pNF, phosphorylated neurofilament; $\beta$-APP, beta-amyloid precursor protein.

5200 Fragment Analyzer (Agilent, Basel, Switzerland). The wild-type allele yielded no amplicon, as the primers can only bind in a tail-to-tail orientation on the genomic segment without the duplication. The duplication allele gave rise to a product of 950 bp, which contains the junction of the two copies. To enable a technical validation of the above-mentioned primers in wild-type animals, additional PCR analyses were performed. Primer F2_DupF was used together with primer R2 for generation of an 861 bp amplicon, while primer R1_DupR was used with primer F1 to produce an amplicon of 889 bp length. Direct Sanger sequencing of the PCR amplicons on an ABI 3730 DNA Analyzer (Thermo Fisher Scientific, Reinach, Switzerland) was performed after treatment with exonuclease I and alkaline phosphatase. Sanger sequences were analyzed using the SEQUENCHER 5.1 software (Gene Codes, Ann Arbor, MI, USA).

# RESULTS

## Histochemistry and immunohistochemistry

The neurons of the CNS of the affected rabbit were characterized by loss, necrosis or a variable accumulation of a finely granular, weakly eosinophilic to yellowish-brown material in the cytoplasm displacing the nucleus and/or Nissl substance to the periphery (Figure 1a). The cytoplasmic storage material stained weakly positive for Sudan black B (Figure 1b) and was negative for Ziehl–Neelsen (Figure 1c). In addition, it exhibited green autofluorescence (Figure 1d). In contrast, there were no comparable changes in the sire of the proband.

Immunohistochemistry demonstrated astrogliosis, microgliosis (Figure 2) and axonal damage (Figure 3). There was a mild to marked proliferation of astrocytes positive for glial fibrillary acidic protein in the CNS, especially in the white matter of the cerebral cortex (Figure 2a,b) and cerebellum, and at the interface of the cerebellar molecular and granular cell layers. Similarly, a slight to moderate increase in plump microglia positive for ionized calcium binding adapter molecule 1 (Iba1) was observed, occurring predominantly in the cerebral cortex (Figure 2c,d). A marked loss of phosphorylated neurofilament (pNF) expression was visible in Purkinje cells (Figure 3a,b), while it was present to varying degrees in the remaining CNS. In addition, a slight to moderate increase in immunolabeling for non-phosphorylated neurofilament (nNF) was observed in the axons of spinal cord, Purkinje cells and cerebellar granule neurons (Figure 3c,d), as well as the white matter of the cerebral cortex and cerebellum compared with the control animal. There was also a mild to moderate decrease in staining intensity for nNF in neurons throughout the CNS owing to the cytoplasmic storage material. Axons positive for beta-amyloid precursor protein were frequently present in the white matter throughout the CNS and at the interface between the molecular and granular cell layers of the cerebellum (Figure 3e,f). The immunohistological findings are summarized for each antibody by brain region in Table 3.

## Genetic analysis

As clinical and histopathological findings resembled previously published cases of humans and companion animals with NCL (Bond et al., 2013; Bullock et al., 2022; Cesta et al., 2006; Chalkley et al., 2014; Faller et al., 2016; Nibe et al., 2011; Nolte et al., 2016; Story et al., 2020), we hypothesized that the phenotype in the affected rabbit was due to a protein changing variant in one of the 13 known NCL candidate genes (Nita et al., 2016).

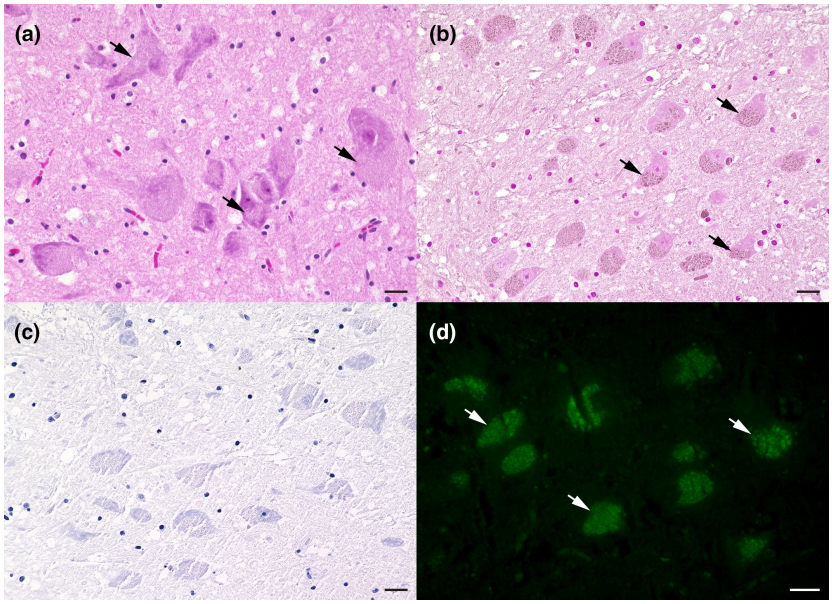


**FIGURE 1** Histochemical findings in the brainstem of a rabbit with neuronal ceroid lipofuscinosis. (a) Accumulation of a cytoplasmic, pale eosinophilic, granular pigment in neurons (arrows) displacing Nissl substance to the periphery. Hematoxylin and eosin. (b) Brown-stained intraneuronal pigment (arrows). Sudan black B. (c) The intraneuronal pigment is negative for Ziehl–Neelsen staining. (d) Green autofluorescence of intraneuronal storage material (arrows), GFP filter, excitation 472.5 ± 30 nm, emission 520 ± 35 nm. All scale bars = 20 μm.

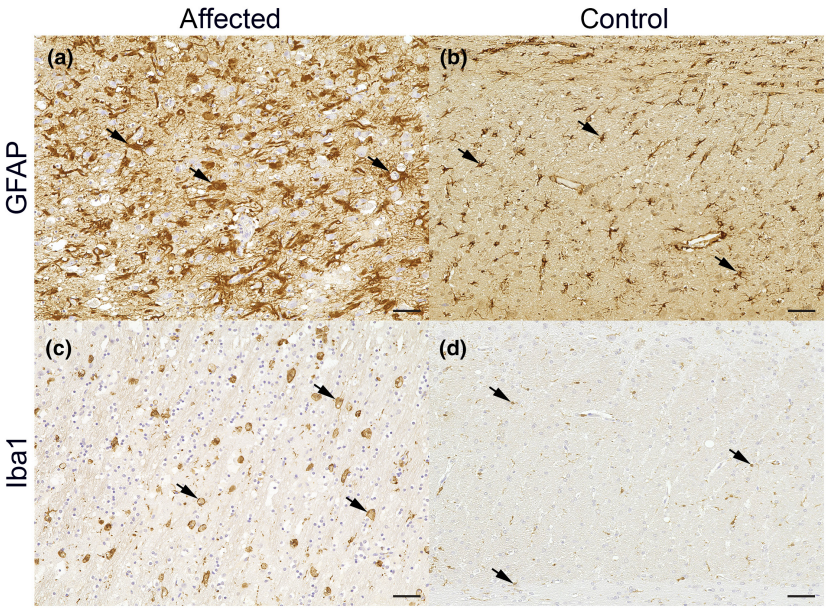


**FIGURE 2** Immunohistochemical findings in the cerebrum of a rabbit with neuronal ceroid lipofuscinosis. (a) The white matter of the cerebral cortex presents conspicuous GFAP immunolabeling for astrocytes with irregular and thickened cell processes (arrows). (b) Immunolabeling for GFAP in the white matter of the cerebral cortex in the control animal. Stained astrocytes appear physiological (arrows). (c) Immunolabeling for Iba1 yields numerous plump, partly vacuolated Iba1-positive microglia (arrows). (d) Unremarkable expression of Iba1 in cerebral microglia of the control animal. GFAP, Glial fibrillary acidic protein; Iba1, ionized calcium binding adapter molecule 1. All scale bars = 50 μm.

The genome of the affected rabbit was sequenced and searched for private heterozygous variants in *DNAJC5* and private homozygous variants in the other 12 known candidate genes. Subsequently, variants that were present in at least one of 12 control rabbits were excluded. Thus, only private variants in the affected rabbit were further considered (Table 4, Table S3).

This analysis did not identify any private protein-changing variants in a functional candidate gene. The automated variant calling pipeline considered only single nucleotide variants and small indels. We therefore performed a visual search for structural variants that would have been missed during the initial analysis and detected a single structural variant involving protein-coding exons among the 13 candidate genes. This variant, NC_013683.1:g.103,727,963_103,738,667dup, represents a duplication of 10 705 bp on chromosome 15 within the *MFSD8* gene (Figure 4). It contains the internal exons 4 and 5 of the gene, XM_002717263.3:c.202_701dup. The presence of the duplication was confirmed in the affected rabbit and its sire by Sanger sequencing of PCR amplicons spanning the junction of the two copies. The duplication was absent in whole genome sequencing data of 12 control rabbits and five additionally genotyped healthy rabbits.

Assuming unaltered splicing of all exons, the duplication of exons 4 and 5 results in a change to the transcript that can be designated as XM_002717263.3:r.(202_701dup). The duplication in the predicted transcript introduces a frameshift and premature stop codon, XP_002717309.2:p.(Glu235Leufs*23), thus truncating 50.8% of the wildtype *MFSD8* coding sequence (Figure 5).

## DISCUSSION

Neuronal ceroid lipofuscinoses comprise one of the most common neurodegenerative diseases of early life (Qureshi et al., 2020). The objective of this study was the histochemical, immunohistological and genetic characterization of a female lionhead dwarf rabbit aged 3 years and 11 months reported with progressive neurological signs reminiscent of NCL. Similar alterations had been clinically observed for the dam of the proband. The dam initially presented with increasing anxiety as a change in behavior, which worsened over the course of the following year from extreme panic to jumping headfirst into objects as a reaction to noises, changes in light or vibrations. In addition, there was severe enuresis. Owing to the rapid progression of the condition and the unfavorable prognosis, the dam was euthanized at the age of approximately 2 years 6 months. The sister of the affected rabbit described in this report died suddenly at the age of 8 years, without any previously known illness. Unfortunately, neither the dam nor the sister were available for necropsy or genetic testing. Like the sire, the sister of the proband was clinically unremarkable in terms of neurological signs throughout her life.

The age of onset of the disease in the case described herein and possibly the dam was between 2 and 3 years of age. There were similarities with regard to the clinical

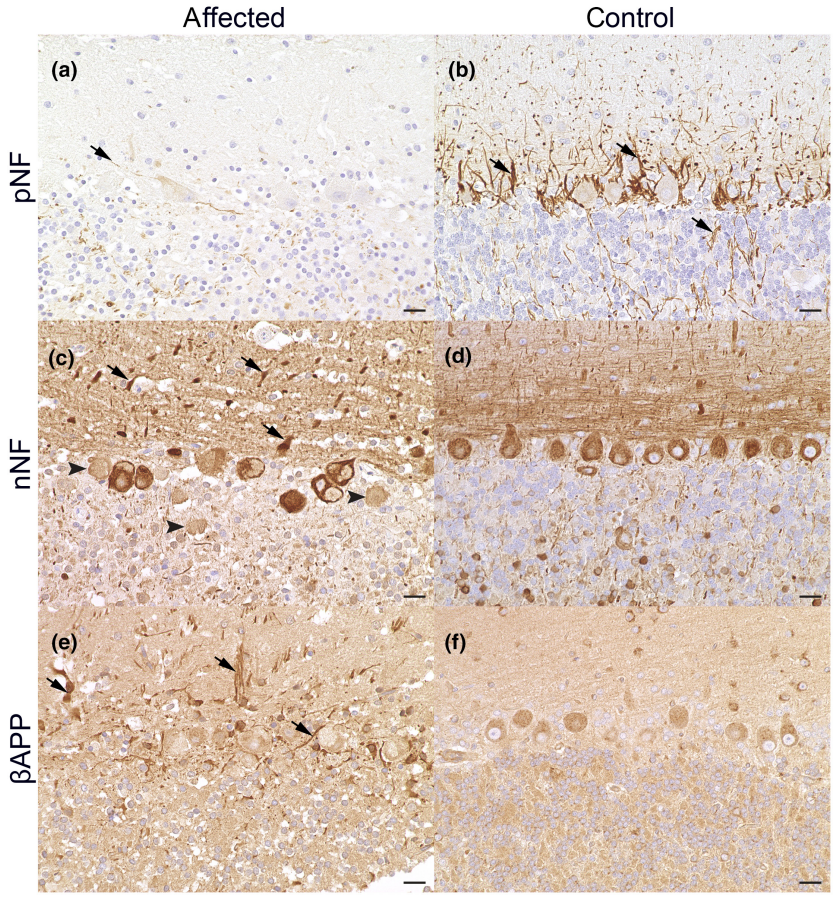


**FIGURE 3** Immunohistochemical findings in the cerebellum of a rabbit with neuronal ceroid lipofuscinosis. (a) Profound loss of pNF in axons (arrows) at the interface between the molecular and granular cell layers. (b) Numerous pNF-positive axons (arrows) at the interface between the molecular and granular cell layers in the control animal. (c) Immunolabeling for non-phosphorylated neurofilament (nNF) shows a mild to moderate loss of expression for nNF in neurons of the granular cell layer and Purkinje cells (arrowheads) with a simultaneous slight to moderate increase in nNF-positive axons (arrows). (d) Prominent immunolabeling for nNF in Purkinje cells and partly in neurons of the granular cell layer in a control animal. (e) Frequent immunolabeling of swollen axons for *β*-APP (arrows) at the interface between the molecular and granular cell layers. (f) Immunolabeling for *β*-APP does not reveal any axonal damage in the control animal. nNF, Non-phosphorylated neurofilament; pNF, phosphorylated neurofilament; *β*-APP, beta-amyloid precursor protein. All scale bars = 20 μm.

**TABLE 3** Immunohistochemical findings in the central nervous system.

| Antibody | Cerebral cortex | Hippocampus | Diencephalon | Cerebellum | Brainstem | Spinal cord |
|---|---|---|---|---|---|---|
| GFAP | ++(+) | ++ | +(+) | ++(+) | + | + |
| Iba1 | ++ | + | +(+) | +(+) | + | + |
| pNF[a] | +(+) | ++ | +(+) | + to +++[b] | +(+) | + |
| nNF[c] | +(+) | + | + | +(+) | +(+) | ++ |
| *β*-APP | +(+) | + | + | +(+) | +(+) | +(+) |

*Note*: +, low numbers (<30%) of immunopositive cells/axons; ++, moderate numbers (30–60%) of immunopositive cells/axons; +++, high numbers (>60%) of immunopositive cells/axons.

Abbreviations: GFAP, glial fibrillary acidic protein; Iba1, ionized calcium binding adapter molecule 1; nNF, non-phosphorylated neurofilament; pNF, phosphorylated neurofilament; *β*-APP, beta-amyloid precursor protein.

[a]The semiquantitative analysis refers here to a loss of immunoreactivity in axons for pNF.

[b]Varies greatly depending on the localization.

[c]The semiquantitative analysis refers here to an increase of immunoreactivity in axons for nNF.

course of NCL in other species such as cognitive changes and vision loss in humans (Schulz et al., 2013) or blindness, pacing, anxiety, disorientation and ataxia in other animal species (Ashwini et al., 2016; Guevar et al., 2020; Guo et al., 2015; McBride et al., 2018). In rabbits, to the best of our knowledge, a similar combination of clinical signs has only been described in a miniature lop pet rabbit with GM2 gangliosidosis, showing behavioral disturbances,

**TABLE 4** Results of variant filtering in the affected rabbit against 12 control genomes.

| Filtering step | Homozygous variants | Heterozygous variants |
|---|---|---|
| All variants in the affected rabbit | 9 013 334 | 11 327 001 |
| Private variants | 78 928 | 210 582 |
| Private protein-changing variants | 158 | 652 |
| Private protein changing variants in NCL candidate genes | 0 | 0 |

Abbreviation: NCL, Neuronal ceroid lipofuscinoses.

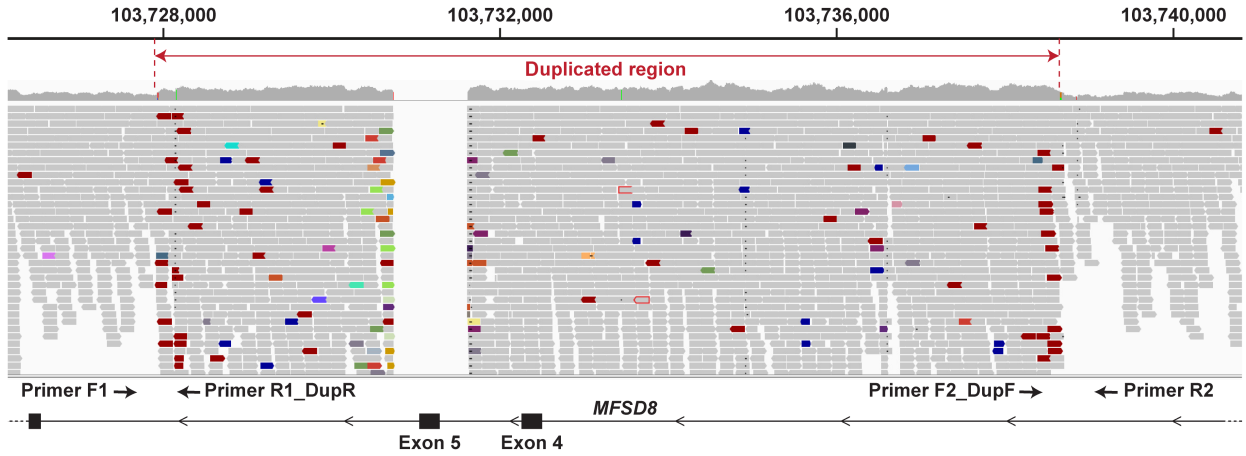


**FIGURE 4** Integrative genomics viewer (IGV) screenshot of the short-read alignments of the affected rabbit illustrating the structural variant. Base pair coordinates refer to chromosome 15 of the OryCun 2.0 genome reference sequence. The affected rabbit shows a ~2-fold increase in coverage in a ~10.7 kb segment. Several read pairs with incorrect read-pair orientation at the boundaries of the duplicated sequence are indicated in dark red. These features are characteristic for a duplication of a genomic segment. The position of four PCR primers used for genotyping the duplication and its breakpoints are indicated. The duplication harbors exons 4 and 5 of *MFSD8*. The region without any mapped reads harboring exon 5 represents a gap in the genome reference assembly.

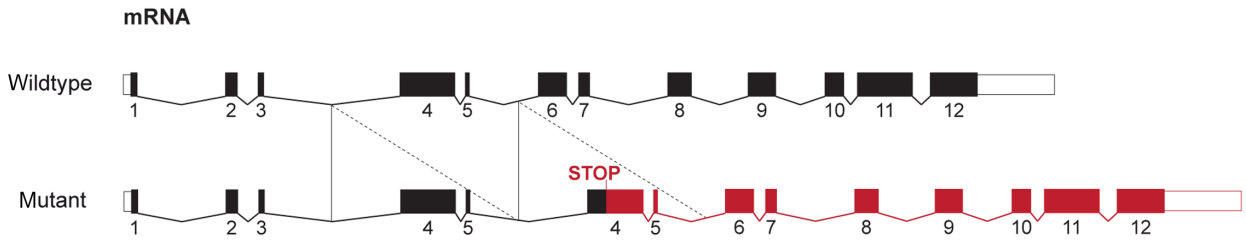


**FIGURE 5** Schematic representation of the predicted consequences of the NC_013683.1:g.103,727,963_103,738,667dup variant on the mRNA level. The duplicated region is indicated by the vertical lines. The dashed lines indicate the position of the duplicated copy. The premature stop codon and downstream sequences are highlighted in red.

bumping into objects and pronounced ataxia, among other symptoms (Rickmeyer et al., 2013), and in Netherland Dwarf rabbits infected with *Enzephalitozoon cuniculi*, showing inter alia ataxia (Doboși et al., 2022).

The histochemical and immunohistological results in the CNS are consistent with previously published reports on NCL in humans (Anderson et al., 2013) and other animal species (Ashwini et al., 2016; Cesta et al., 2006; Chalkley et al., 2014; Faller et al., 2016; Guo et al., 2015; Nibe et al., 2011; Nolte et al., 2016). The most prominent features in this case were the astrogliosis and loss of phosphorylated neurofilament throughout the CNS.

In addition to the changes in the CNS, an accumulation of ceroid lipofuscin in the retina leading to degenerative changes and progressive vision loss has been described in other animals with NCL (Ashwini et al., 2016; Faller et al., 2016; McBride et al., 2018). Interestingly, no ceroid-lipofuscin pigment or degenerative changes were detected in the retina of the affected rabbit described herein, indicating a neurogenic cause for the vision loss observed.

We identified a ~10.7 kb genomic duplication on chromosome 15 harboring exons 4 and 5 of the *MFSD8* gene in the rabbit with NCL. *MFSD8* encodes the major facilitator superfamily domain containing protein 8 (MFSD8), which is an integral lysosomal transmembrane protein (Siintola et al., 2007). It has 12 membrane spanning domains and localizes to lysosomes and late endosomes in neurons (Sharifi et al., 2010). Human patients with variants in this gene develop NCL7 (Siintola et al., 2007). To date, at least 38 different disease-associated *MFSD8* variants have been reported in human medicine (Mole et al., 2019). Various murine disease models have been developed and studied (Brandenstein et al., 2016; Damme et al., 2014). However, the complete function of MFSD8 is not yet fully understood (Specchio et al., 2021). In veterinary medicine, candidate causative genetic variants for NCL7 have been reported in dogs (Ashwini et al., 2016; Faller et al., 2016; Guo et al., 2015; Karli et al., 2016), a single cat (Guevar et al., 2020) and non-human primates (McBride et al., 2018).

The mutant allele was detected neither in whole genome sequences of 12 control rabbits nor in any of the five additionally genotyped unrelated controls. In the affected rabbit, whole-genome sequencing showed homozygosity for the identified ~10.7 kb duplication via a two-fold increase in coverage. Determination of zygosity in the sire was not possible using conventional PCR amplification. The mutant allele was amplified, but the presence of the wild-type allele was not verified. However, the sire was assumed to be heterozygous as it was clinically and pathomorphologically inconspicuous for NCL. *MFSD8* variants usually only cause disease when present biallelically (Siintola et al., 2007).

The identified variant is predicted to result in a frameshift and premature stop codon in MFSD8, XP_002717309.2:p.(Glu235Leufs*23). Transcripts with premature stop codons are frequently degraded by nonsense-mediated mRNA decay with absent protein expression (Wei-Lin Popp & Maquat, 2013). Experimental confirmation at the mRNA level would be required to confirm the predicted nonsense mediated decay of the transcript.

In conclusion, our study provides a greatly refined phenotypic characterization of the rabbit originally described in Böttcher-Künneke et al. (2020). To the best of our knowledge, we provide the first report of a genetically characterized NCL in a rabbit. These findings provide further support for the functional conservation of *MFSD8* in different mammalian species.

## AUTHOR CONTRIBUTIONS

**Matthias Christen:** Investigation; visualization; writing – original draft; writing – review and editing. **Katharina M. Gregor:** Investigation; visualization; writing – original draft; writing – review and editing. **Ariane Böttcher-Künneke:** Investigation; writing – original draft; writing – review and editing. **Mara S. Lombardo:** Investigation; writing – review and editing. **Wolfgang Baumgärtner:** Conceptualization; supervision; writing – review and editing. **Vidhya Jagannathan:** Data curation; writing – review and editing. **Christina Puff:** Conceptualization; investigation; supervision; visualization; writing – original draft; writing – review and editing. **Tosso Leeb:** Conceptualization; supervision; visualization; writing – original draft; writing – review and editing.

## ACKNOWLEDGEMENTS

Sincere thanks are given to the owner Lara Balzer for providing the animals and preclinical information. The authors thank Julia Baskas, Petra Grünig, Dunja Hoffmann, Siegfried Jelitto, Caroline Schütz and Nathalie Besuchet-Schmutz for their excellent technical support. Stefan Rietmann is acknowledged for help during the revision of the manuscript. We also thank the Next Generation Sequencing Platform of the University of Bern for performing the high-throughput experiments and the Interfaculty Bioinformatics Unit of the University of Bern for providing high-performance computing infrastructure. Open access funding provided by Universitat Bern.

## CONFLICT OF INTEREST STATEMENT

The authors declare no conflicts of interest.

## DATA AVAILABILITY STATEMENT

All data are contained within the manuscript and its Supporting Information. Accession numbers of the whole genome sequences used in this study are listed in Table S2.

## ETHICS STATEMENT

All examinations were executed with written informed owner's consent according to ethical guidelines of the University of Veterinary Medicine, Hannover.

## ORCID

*Matthias Christen* https://orcid.org/0000-0003-3275-5929
*Katharina M. Gregor* https://orcid.org/0009-0005-1270-312X
*Ariane Böttcher-Künneke* https://orcid.org/0009-0002-5777-6056
*Mara S. Lombardo* https://orcid.org/0009-0007-1643-1795
*Wolfgang Baumgärtner* https://orcid.org/0000-0001-8151-5644
*Vidhya Jagannathan* https://orcid.org/0000-0002-8155-0041
*Christina Puff* https://orcid.org/0000-0002-2592-6868
*Tosso Leeb* https://orcid.org/0000-0003-0553-4880

## REFERENCES

Amberger, J.S., Bocchini, C.A., Schiettecatte, F., Scott, A.F. & Hamosh, A. (2015) OMIM.org: Online Mendelian Inheritance

in Man (OMIM®), an online catalog of human genes and genetic disorders. *Nucleic Acids Research*, 43(Database issue), D789–D798. Available from: https://doi.org/10.1093/nar/gku1205

Anderson, G.W., Goebel, H.H. & Simonati, A. (2013) Human pathology in NCL. *Biochimica et Biophysica Acta*, 1832(11), 1807–1826. Available from: https://doi.org/10.1016/j.bbadis.2012.11.014

Ashwini, A., D'Angelo, A., Yamato, O., Giordano, C., Cagnotti, G., Harcourt-Brown, T. et al. (2016) Neuronal ceroid lipofuscinosis associated with an MFSD8 mutation in Chihuahuas. *Molecular Genetics and Metabolism*, 118(4), 326–332. Available from: https://doi.org/10.1016/j.ymgme.2016.05.008

Barker, E., Morgan, A. & Barclay, J.W. (2023) A *Caenorhabditis elegans* model of autosomal dominant adult-onset neuronal ceroid lipofuscinosis identifies ethosuximide as a potential therapeutic. *Human Molecular Genetics*, 32(11), 1772–1785. Available from: https://doi.org/10.1093/hmg/ddac263

Bond, M., Holthaus, S.-M.K., Tammen, I., Tear, G. & Russell, C. (2013) Use of model organisms for the study of neuronal ceroid lipofuscinosis. *Biochimica et Biophysica Acta (BBA) – Molecular Basis of Disease*, 1832(11), 1842–1865. Available from: https://doi.org/10.1016/j.bbadis.2013.01.009

Böttcher-Künneke, A., Gregor, K., Baumgärtner, W. & Puff, C. (2020) Neuronale Speicherkrankheit bei einem ausgewachsenen weiblichen Kaninchen. *Kleintierpraxis*, 65(12), 656–665. Available from: https://doi.org/10.2377/0023-2076-65-656

Brandenstein, L., Schweizer, M., Sedlacik, J., Fiehler, J. & Storch, S. (2016) Lysosomal dysfunction and impaired autophagy in a novel mouse model deficient for the lysosomal membrane protein Cln7. *Human Molecular Genetics*, 25(4), 777–791. Available from: https://doi.org/10.1093/hmg/ddv615

Bullock, G., Johnson, G.S., Mhlanga-Mutangadura, T., Petesch, S.C., Thompson, S., Goebbels, S. et al. (2022) Lysosomal storage disease associated with a CNP sequence variant in Dalmatian dogs. *Gene*, 830, 146513. Available from: https://doi.org/10.1016/j.gene.2022.146513

Cesta, M.F., Mozzachio, K., Little, P.B., Olby, N.J., Sills, R.C. & Brown, T.T. (2006) Neuronal ceroid lipofuscinosis in a Vietnamese potbellied pig (*Sus scrofa*). *Veterinary Pathology*, 43(4), 556–560. Available from: https://doi.org/10.1354/vp.43-4-556

Chalkley, M.D., Armien, A.G., Gilliam, D.H., Johnson, G.S., Zeng, R., Wünschmann, A. et al. (2014) Characterization of neuronal ceroid-lipofuscinosis in 3 cats. *Veterinary Pathology*, 51(4), 796–804. Available from: https://doi.org/10.1177/0300985813502818

Cingolani, P., Platts, A., Wang, L.L., Coon, M., Nguyen, T., Wang, L. et al. (2012) A program for annotating and predicting the effects of single nucleotide polymorphisms, SnpEff. *Fly*, 6(2), 80–92. Available from: https://doi.org/10.4161/fly.19695

Damme, M., Brandenstein, L., Fehr, S., Jankowiak, W., Bartsch, U., Schweizer, M. et al. (2014) Gene disruption of Mfsd8 in mice provides the first animal model for CLN7 disease. *Neurobiology of Disease*, 65, 12–24. Available from: https://doi.org/10.1016/j.nbd.2014.01.003

Doboși, A.A., Bel, L.V., Paștiu, A.I. & Pusta, D.L. (2022) A review of *Encephalitozoon cuniculi* in domestic rabbits (*Oryctolagus cuniculus*) – biology, clinical signs, diagnostic techniques, treatment, and prevention. *Pathogens*, 11(12), 1486. Available from: https://doi.org/10.3390/pathogens11121486

Faller, K.M.E., Bras, J., Sharpe, S.J., Anderson, G.W., Darwent, L., Kun-Rodrigues, C. et al. (2016) The Chihuahua dog: a new animal model for neuronal ceroid lipofuscinosis CLN7 disease? *Journal of Neuroscience Research*, 94(4), 339–347. Available from: https://doi.org/10.1002/jnr.23710

Guevar, J., Hug, P., Giebels, F., Durand, A., Jagannathan, V. & Leeb, T. (2020) A major facilitator superfamily domain 8 frameshift variant in a cat with suspected neuronal ceroid lipofuscinosis. *Journal of Veterinary Internal Medicine*, 34(1), 289–293. Available from: https://doi.org/10.1111/jvim.15663

Guo, J., Johnson, G.S., Cook, J., Harris, O.K., Mhlanga-Mutangadura, T., Schnabel, R.D. et al. (2019) Neuronal ceroid lipofuscinosis in a German shorthaired pointer associated with a previously reported CLN8 nonsense variant. *Molecular Genetics and Metabolism Reports*, 21, 100521. Available from: https://doi.org/10.1016/j.ymgmr.2019.100521

Guo, J., O'Brien, D.P., Mhlanga-Mutangadura, T., Olby, N.J., Taylor, J.F., Schnabel, R.D. et al. (2015) A rare homozygous MFSD8 single-base-pair deletion and frameshift in the whole genome sequence of a Chinese crested dog with neuronal ceroid lipofuscinosis. *BMC Veterinary Research*, 10(1), 960. Available from: https://doi.org/10.1186/s12917-014-0181-z

Huang, B., Zdora, I., de Buhr, N., Lehmbecker, A., Baumgärtner, W. & Leitzen, E. (2021) Phenotypical peculiarities and species-specific differences of canine and murine satellite glial cells of spinal ganglia. *Journal of Cellular and Molecular Medicine*, 25(14), 6909–6924. Available from: https://doi.org/10.1111/jcmm.16701

Huber, R.J., Hughes, S.M., Liu, W., Morgan, A., Tuxworth, R.I. & Russell, C. (2020) The contribution of multicellular model organisms to neuronal ceroid lipofuscinosis research. *Biochimica et Biophysica Acta – Molecular Basis of Disease*, 1866(9), 165614. Available from: https://doi.org/10.1016/j.bbadis.2019.165614

Jagannathan, V., Drögemüller, C., Leeb, T., Aguirre, G., André, C., Bannasch, D. et al. (2019) A comprehensive biomedical variant catalogue based on whole genome sequences of 582 dogs and eight wolves. *Animal Genetics*, 50(6), 695–704. Available from: https://doi.org/10.1111/age.12834

Karli, P., Oevermann, A., Bauer, A., Jagannathan, V. & Leeb, T. (2016) MFSD8 single-base pair deletion in a Chihuahua with neuronal ceroid lipofuscinosis. *Animal Genetics*, 47(5), 631. Available from: https://doi.org/10.1111/age.12449

Katz, M.L., Buckley, R.M., Biegen, V., O'Brien, D.P., Johnson, G.C., Warren, W.C. et al. (2020) Neuronal ceroid lipofuscinosis in a domestic cat associated with a DNA sequence variant that creates a premature stop codon in CLN6. *G3: Genes, Genomes, Genetics*, 10(8), 2741–2751. Available from: https://doi.org/10.1534/g3.120.401407

McBride, J.L., Neuringer, M., Ferguson, B., Kohama, S.G., Tagge, I.J., Zweig, R.C. et al. (2018) Discovery of a CLN7 model of Batten disease in non-human primates. *Neurobiology of Disease*, 119, 65–78. Available from: https://doi.org/10.1016/j.nbd.2018.07.013

McKenna, A., Hanna, M., Banks, E., Sivachenko, A., Cibulskis, K., Kernytsky, A. et al. (2010) The Genome Analysis Toolkit: a MapReduce framework for analyzing next-generation DNA sequencing data. *Genome Research*, 20(9), 1297–1303. Available from: https://doi.org/10.1101/gr.107524.110

Mole, S.E., Anderson, G., Band, H.A., Berkovic, S.F., Cooper, J.D., Kleine Holthaus, S.-M. et al. (2019) Clinical challenges and future therapeutic approaches for neuronal ceroid lipofuscinosis. *The Lancet Neurology*, 18(1), 107–116. Available from: https://doi.org/10.1016/S1474-4422(18)30368-5

Nibe, K., Miwa, Y., Matsunaga, S., Chambers, J.K., Uetsuka, K., Nakayama, H. et al. (2011) Clinical and pathologic features of neuronal ceroid-lipofuscinosis in a ferret (*Mustela putorius furo*). *Veterinary Pathology*, 48(6), 1185–1189. Available from: https://doi.org/10.1177/0300985811400441

Nicholas, F., Tammen, I. & Sydney Informatics Hub. (1995) *Online Mendelian inheritance in animals (OMIA)*. Sydney, NSW: The University of Sydney. Available from: https://doi.org/10.25910/2amr-pv70

Nita, D.A., Mole, S.E. & Minassian, B.A. (2016) Neuronal ceroid lipofuscinoses. *Epileptic Disorders*, 18(S2), 73–88. Available from: https://doi.org/10.1684/epd.2016.0844

Nittari, G., Tomassoni, D., Roy, P., Martinelli, I., Tayebati, S.K. & Amenta, F. (2023) Batten disease through different in vivo and in vitro models: a review. *Journal of Neuroscience Research*, 101(3), 298–315. Available from: https://doi.org/10.1002/jnr.25147

Nolte, A., Bello, A., Drögemüller, M., Leeb, T., Brockhaus, E., Baumgärtner, W. et al. (2016) Neuronal ceroid lipofuscinosis in an adult American Staffordshire terrier. *Tierarztliche Praxis Ausgabe K: Kleintiere/Heimtiere*, 44(6), 431–437. Available from: https://doi.org/10.15654/TPK-150766

Parenti, G., Andria, G. & Ballabio, A. (2015) Lysosomal storage diseases: from pathophysiology to therapy. *Annual Review of Medicine*, 66(1), 471–486. Available from: https://doi.org/10.1146/annurev-med-122313-085916

Platt, F.M., D'Azzo, A., Davidson, B.L., Neufeld, E.F. & Tifft, C.J. (2018) Lysosomal storage diseases. *Nature Reviews Disease Primers*, 4(1), 27. Available from: https://doi.org/10.1038/s41572-018-0025-4

Qureshi, Y.H., Baez, P. & Reitz, C. (2020) Endosomal trafficking in Alzheimer's disease, Parkinson's disease, and neuronal ceroid lipofuscinosis. *Molecular and Cellular Biology*, 40(19), 1–12. Available from: https://doi.org/10.1128/MCB.00262-20

Rickmeyer, T., Schöniger, S., Petermann, A., Harzer, K., Kustermann-Kuhn, B., Fuhrmann, H. et al. (2013) GM2 gangliosidosis in an adult pet rabbit. *Journal of Comparative Pathology*, 148(2–3), 243–247. Available from: https://doi.org/10.1016/j.jcpa.2012.06.008

Robles, L.J. (1978) Accumulation and identification of lipofuscin-like pigment in the neurons of *Bulla gouldiana* (Gastropoda: Opisthobranchia). *Mechanisms of Ageing and Development*, 7(1), 53–64. Available from: https://doi.org/10.1016/0047-6374(78)90052-0

Schulz, A., Kohlschütter, A., Mink, J., Simonati, A. & Williams, R. (2013) NCL diseases – clinical perspectives. *Biochimica et Biophysica Acta*, 1832(11), 1801–1806. Available from: https://doi.org/10.1016/j.bbadis.2013.04.008

Sharifi, A., Kousi, M., Sagné, C., Bellenchi, G.C., Morel, L., Darmon, M. et al. (2010) Expression and lysosomal targeting of CLN7, a major facilitator superfamily transporter associated with variant late-infantile neuronal ceroid lipofuscinosis. *Human Molecular Genetics*, 19(22), 4497–4514. Available from: https://doi.org/10.1093/hmg/ddq381

Siintola, E., Topcu, M., Aula, N., Lohi, H., Minassian, B.A., Paterson, A.D. et al. (2007) The novel neuronal ceroid lipofuscinosis gene MFSD8 encodes a putative lysosomal transporter. *The American Journal of Human Genetics*, 81(1), 136–146. Available from: https://doi.org/10.1086/518902

Specchio, N., Ferretti, A., Trivisano, M., Pietrafusa, N., Pepi, C., Calabrese, C. et al. (2021) Neuronal ceroid lipofuscinosis: potential for targeted therapy. *Drugs*, 81(1), 101–123. Available from: https://doi.org/10.1007/s40265-020-01440-7

Story, B.D., Miller, M.E., Bradbury, A.M., Million, E.D., Duan, D., Taghian, T. et al. (2020) Canine models of inherited musculoskeletal and neurodegenerative diseases. *Frontiers in Veterinary Science*, 7, 1–21. Available from: https://doi.org/10.3389/fvets.2020.00080

Swier, V.J., White, K.A., Johnson, T.B., Sieren, J.C., Johnson, H.J., Knoernschild, K. et al. (2022) A novel porcine model of CLN2 batten disease that recapitulates patient phenotypes. *Neurotherapeutics*, 19(6), 1905–1919. Available from: https://doi.org/10.1007/s13311-022-01296-7

Villani, N.A., Bullock, G., Michaels, J.R., Yamato, O., O'Brien, D.P., Mhlanga-Mutangadura, T. et al. (2019) A mixed breed dog with neuronal ceroid lipofuscinosis is homozygous for a CLN5 nonsense mutation previously identified in Border Collies and Australian cattle dogs. *Molecular Genetics and Metabolism*, 127(1), 107–115. Available from: https://doi.org/10.1016/j.ymgme.2019.04.003

Wei-Lin Popp, M. & Maquat, L.E. (2013) Organizing principles of mammalian nonsense-mediated mRNA decay. *Annual Review of Genetics*, 47, 139–165. Available from: https://doi.org/10.1146/annurev-genet-111212-133424

Ziehl, F. (1882) Zur Färbung des Tuberkelbacillus. *DMW – Deutsche Medizinische Wochenschrift*, 8(33), 451. Available from: https://doi.org/10.1055/s-0029-1196721

## SUPPORTING INFORMATION

Additional supporting information can be found online in the Supporting Information section at the end of this article.

**How to cite this article:** Christen, M., Gregor, K.M., Böttcher-Künneke, A., Lombardo, M.S., Baumgärtner, W., Jagannathan, V. et al. (2024) Intragenic *MFSD8* duplication and histopathological findings in a rabbit with neuronal ceroid lipofuscinosis. *Animal Genetics*, 55, 588–598. Available from: https://doi.org/10.1111/age.13441